MIMO Fuzzy Control Solutions for the Level Control of Vertical Two Tank Systems

Claudia-Adina Bojan-Dragoş, Elena-Lorena Hedrea, Radu-Emil Precup,
Alexandra-Iulia Szedlak-Stinean and Raul-Cristian Roman
Department of Automation and Applied Informatics, Politehnica University Timisoara, Bd. V. Parvan 2, Timisoara, Romania

Keywords: Vertical Two Tank Systems, MIMO Fuzzy Control, Nonlinear System, Experimental Results.

Abstract: The paper presents the design and validation of two control system (CS) structures for the level control of vertical two tank systems. The first CS structure consists of a Multi Input Multi Output Proportional Integral Fuzzy Controller with integration of controller input (MIMO–PI–FC–II) and the second CS structure consists of a Multi Input Multi Output Proportional Integral Fuzzy Controller with integration of controller output (MIMO–PI–FC–OI). The suggested CS structures are designed using the modulus optimum method and the modal equivalence principle. The experimental results validate the proposed control solutions. Finally a comparative analysis is also included.

1 INTRODUCTION

The vertical two-tank systems (V2TS) benchmark is a nonlinear Multi Input-Multi Output process. An overview of some recent control structures for the level control in the two-tank systems includes: the popular Proportional-Integral-Derivative (PID) control (Dormido et al., 2008) neural networks (Na et al., 2012), IFT–based linear and fuzzy control (Precup et al., 2010), (Precup et al., 2013), switched model predictive control (Mirzaee and Salahshoor, 2012), robust and fuzzy predictive control (Bouzouita et al., 2008), gain-scheduling control (Chakravarthi et al., 2014), (Dinesh Kumar and Meenakshipriya, 2012) or sliding mode control (Orani, 2009).

This paper is focused on the development of two control system (CS) structures for the level control of two tanks of vertical two tank systems. The first CS structure consists of a Multi Input Multi Output Proportional Integral Fuzzy Controller with integration of controller input (MIMO–PI–FC–II) and the second CS structure consists of a Multi Input Multi Output Proportional Integral Fuzzy Controller with integration of controller output (MIMO–PI–FC–OI).

The paper is organized as follows: the nonlinear model and the identified two-order benchmark-type transfer functions (t.f.s) of the simplified models of V2TS are given in Section 2. The proposed CS structures are next developed in Section 3, and the comparative study and the experimental results are presented in Section 4. The conclusions are highlighted in Section 5.

2 PROCESS MATHEMATICAL MODELING

The V2TS is designed as a laboratory equipment that allows for convenient experiments. The process models consist of the following first principles state–space equations of the process (Inteco, 2007):

$$\begin{aligned}\dot{H}_1 &= q/(a\,w) - R_1 H_1^{\alpha_1}/(a\,w),\\ \dot{H}_2 &= R_1 H_1^{\alpha_1}/(c\,w + (H_2/H_{2\max})b\,w)\\ &\quad - R_2 H_2^{\alpha_2}/(c\,w + (H_2/H_{2\max})b\,w),\\ y_{H1} &= H_1, y_{H2} = H_2,\end{aligned} \tag{1}$$

where $q = k_{EE}u_1$ is the inflow in time, u_1 is the control input of the first tank, $k_{EE} = 1.6 \cdot 10^{-4}$, H_i, $i = \overline{1,2}$, is the fluid level of i^{th} tank, α_i, $i = \overline{1,2}$, is the flow coefficient for i^{th} tank, R_i, $i = \overline{1,2}$, is the resistance of the output orifice of i^{th} tank, $\beta_i(H_i)$, $i = \overline{1,2}$, is the cross sectional area of i^{th} tank computed at the level

Bojan-Dragoş, C., Hedrea, E., Precup, R., Szedlak-Stinean, A. and Roman, R.
MIMO Fuzzy Control Solutions for the Level Control of Vertical Two Tank Systems.
DOI: 10.5220/0007978508100817
In *Proceedings of the 16th International Conference on Informatics in Control, Automation and Robotics (ICINCO 2019)*, pages 810-817
ISBN: 978-989-758-380-3

H_i, y_{Hi}, $i=\overline{1,2}$ is the measured fluid level, and $u_2 = R_1$ is the control input of the second tank. The block diagram of linear V2TS is given in Fig. 1.

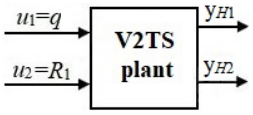

Figure 1: The block diagram of linear V2TS models.

The parameters have the following numerical values: $R_1 = 11.08 \cdot 10^{-5}$, $R_2 = 8.78 \cdot 10^{-5}$, $\alpha_1 = \alpha_2 = 0.5$, $a = 0.25$, $b = 0.345$, $c = 0.1$, $w = 0.035$, $q = 0.435 \cdot 10^{-4}$, $H_{1\max} = H_{2\max} = 0.35 \cdot$

In order to design the proposed control solutions, the nonlinear state-space equations (1) were approximated to two second–order benchmark-type t.f.s using a simple least–squares–based experimental approximation of V2TS (Bojan-Dragos et al., 2018) and considering zero initial conditions:

$$H_{P_{H_1}}(s) = \frac{y_{H1}(s)}{u_1(s)} = \frac{k_{PC_{H_1}}}{(1+T_{1H_1}s)(1+T_{2H_1}s)},$$
$$H_{P_{H_2}}(s) = \frac{y_{H2}(s)}{u_2(s)} = \frac{k_{PC_{H2}}}{(1+T_{1H_2}s)(1+T_{2H_2}s)} \quad (2)$$

where $k_{PC_{H_1}} = 0.26, k_{PC_{H_2}} = 0.25$ are the controlled process gains and $T_{1H_1} = 72, T_{2H_1} = 57, T_{1H_2} = 100$, $T_{2H_2} = 50$ are the time constants.

Using the t.f.s. (2), the following state-space matrices $\mathbf{A}_j, \mathbf{B}_j, \mathbf{C}_j, j \in \{H_1, H_2\}$ are obtained:

$$\mathbf{A}_{H_1} = \begin{bmatrix} -0.32 \cdot 10^{-2} & -0.24 \cdot 10^{-4} \\ 1 & 0 \end{bmatrix}, \mathbf{B}_{H_1} = \begin{bmatrix} 1 \\ 0 \end{bmatrix},$$
$$\mathbf{C}_{H_1} = \begin{bmatrix} 0 & 0.64 \cdot 10^{-5} \end{bmatrix},$$
$$\mathbf{A}_{H_2} = \begin{bmatrix} -0.03 & -0.2 \cdot 10^{-3} \\ 1 & 0 \end{bmatrix}, \mathbf{B}_{H_2} = \begin{bmatrix} 1 \\ 0 \end{bmatrix}, \quad (3)$$
$$\mathbf{C}_{H_2} = \begin{bmatrix} 0 & 0.52 \cdot 10^{-4} \end{bmatrix}$$

3 DESIGN OF LEVEL CONTROL SOLUTIONS

In order to obtain the desired liquid level of the two tanks, H_1 and H_2, two types of fuzzy control structures, namely MIMO PI fuzzy controller with integration of controller input (MIMO–PI–FC–II) and MIMO PI fuzzy controller with integration of controller output (MIMO–PI–FC–OI) were designed in the following paragraphs.

3.1 Design of MIMO PI Fuzzy Controller with Integration of Controller Input (PI-FC-II)

The block diagram of the control structure with MIMO–PI–FC–II is illustrated in Fig. 2, where w_{Hik}, $i=\overline{1,2}$ is the reference input, e_{Hik}, $i=\overline{1,2}$ is the control error, e_{HiIk}, $i=\overline{1,2}$ is the integral of control error, u_{ik}, $i=\overline{1,2}$ is the control input, y_{Hik}, $i=\overline{1,2}$ is the controlled output.

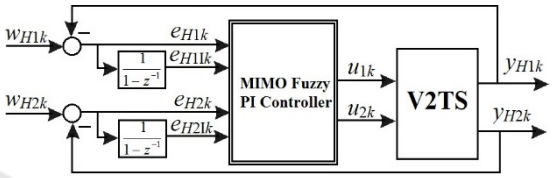

Figure 2: Block diagram MIMO–PI–FC–IICS.

The PI-FC-II design is formulated from the continuous-time PI controller design:

$$H_{C_{Hi}}(s) = [k_{C_{Hi}}/(sT_{c_{Hi}})](1+sT_{c_{Hi}}), i \in \{1,2\} \quad (4)$$

where: $k_{C_{Hi}}$ – gain and $T_{c_{Hi}}$ – integral time constant.

Tustin's method with $T_s = 0.01\,\mathrm{s}$ was used in order to discretize this PI controller and the obtained quasi-continuous digital PI controller is:

$$\begin{aligned} u_{ik} &= K_{I\,Hi}\, e_{Hi\,Ik} + K_{P\,Hi}\, e_{Hi\,k} \\ &= K_{I\,Hi}\,[e_{Hi\,Ik} + (1/\alpha_{Hi})e_{Hi\,k}], i \in \{1,2\} \end{aligned} \quad (5)$$

where the expressions of the PI controller tuning parameters, K_{PHi} and K_{IHi}, are

$$K_{PHi} = k_{C_{Hi}}[1 - T_s/(2T_{c_{Hi}})], K_{IHi} = k_{C_{Hi}} T_s / T_{c_{Hi}},$$
$$\alpha_{Hi} = K_{IHi}/K_{PHi} = 2T_s/(2T_{c_{Hi}} - T_s) \quad (6)$$

The fuzzification employs two linguistic terms with trapezoidal membership functions for the input variables, e_{Hik} and e_{HiIk}, $i=\overline{1,2}$, and four linguistic terms with triangular and trapezoidal membership functions for the output variables, u_{ik}, $i=\overline{1,2}$. The membership functions are given in Fig. 3 and Fig.4. The parameters of MIMO–PI–FC–II block $B_{eHi}, B_{eIHi} = (1/\alpha)B_{eHi}, B_{uHi} = K_{PHi}\,B_{eHi}$, $i=\overline{1,2}$, are chosen based on the modal equivalence principle and the value of the parameter $B_e > 0$ can be set using

the experience of the CS designer, but the stability of the fuzzy control system is used in this paper in this regard.

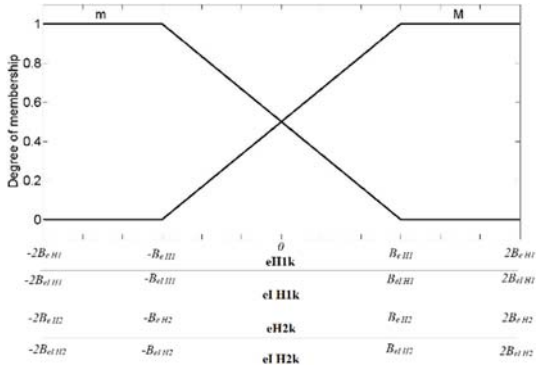

Figure 3: Membership functions of the inputs, e_{Hik} and e_{HiIk}, $i=\overline{1,2}$.

The inference engine employs Mamdani's MAX-MIN compositional rule of inference assisted by the rule base presented in Table 1, which gives the unified rule bases of both PI-FC-OI and PI-FC-II. The centre of gravity method is used for defuzzification in both cases (PI-FC-OI or PI-FC-II).

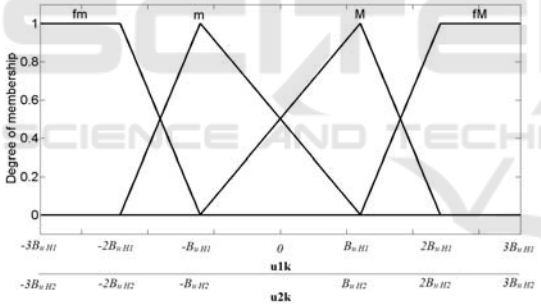

Figure 4: Membership functions of the outputs u_{ik}, $i=\overline{1,2}$.

3.2 Design of MIMO PI Fuzzy Controller with Integration of Controller Output (PI-FC-OI)

The block diagram of the control structure with MIMO–PI–FC–OI is illustrated in Fig. 5, where w_{Hik}, $i=\overline{1,2}$ is the reference input, e_{Hik}, $i=\overline{1,2}$ is the control error, Δe_{Hik}, $i=\overline{1,2}$ is the increment of control error, Δu_{ik}, $i=\overline{1,2}$ is the increment of the control input, u_{ik}, $i=\overline{1,2}$ is the control input, y_{Hik}, $i=\overline{1,2}$ is the controlled output. As shown in Fig. 2 and Fig. 5, the input variables are also scheduling variables of both PI-FC-II and PI-FC-OI.

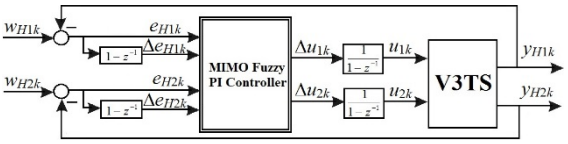

Figure 5: Block diagram MIMO–PI–FC–OICS.

The PI-FC-OI design is formulated from the PI controller design with the t.f. expression given in (4). Tustin's method with $T_s = 0.01\,\mathrm{s}$ was used in order to discretize the continuous-time PI controllers and the following quasi-continuous digital PI controller is obtained:

$$\begin{aligned}\Delta u_{ik} &= K_{PHi}\,\Delta e_{Hik} + K_{IHi}\,e_{Hik} \\ &= K_{PHi}\,(\Delta e_{Hik} + \alpha_{Hi}\,e_{Hik})\end{aligned} \tag{7}$$

where the expressions of the PI controller tuning parameters, K_{PHi} and K_{IHi}, are

$$\begin{aligned}&K_{PHi} = k_{C_{Hi}}[1 - T_s/(2T_{C_{Hi}})],\ K_{IHi} = k_{C_{Hi}}\,T_s/T_{c_{Hi}}, \\ &\alpha_{Hi} = K_{IHi}/K_{PHi} = 2T_s/(2T_{C_{Hi}} - T_s)\end{aligned} \tag{8}$$

The fuzzification, the inference engine and the defuzzification are done in similar manner as in case

Table 1: Decision table of PI-FC-II.

u_{1k} / u_{2k}				e_{H1k}			
				m		M	
				e_{H1Ik}			
				m	M	m	M
e_{H2k}	m	e_{H2Ik}	m	fm / fm	fm / fm	M / M	M / M
			M	fm / fm	fm / fm	M / M	M / M
	M		m	m / m	m / m	FM / FM	FM / FM
			M	m / m	m / m	FM / FM	FM / FM

of MIMO–PI–FC–II. The fuzzification employs two linguistic terms with trapezoidal membership functions for the input variables, e_{Hik} and Δe_{Hik}, $i=\overline{1,2}$ and four linguistic terms with triangular and trapezoidal membership functions for the output variables, Δu_{ik}, $i=\overline{1,2}$. The membership functions are similar to the ones given in Fig. 3 and Fig.4.

The parameters of MIMO–PI–FC–OI block $B_{e\,Hi}$, $B_{\Delta e\,Hi}=\alpha B_{e\,Hi}$, $B_{\Delta u\,Hi}=K_{I\,Hi}\,B_{e\,Hi}$, $i=\overline{1,2}$, are chosen based on the modal equivalence principle, and the value of the parameter $B_e>0$ can be set using the experience of the CS designer, but firstly it must be chosen to ensure the fuzzy CS stability as shown in the next section or using other results as, for instance, those given in (Precup et al., 2014).

3.3 Stability Analysis

For performing the stability analysis, the dynamics of the fuzzy controller is transferred to the process, and this leads to the extended controlled process (EP), illustrated in Fig. 6 (Precup and Preitl, 1997), where $a \in \{j, o\}$ - the upper index corresponding to the type of integration: $a=o$ for integration on the output of the fuzzy controller (for PI-FC-OI), $a=j$ for integration on the input of the fuzzy controller (for PI-FC-II), $\mathbf{w}_{Hik}^{j}=\begin{bmatrix} w_{Hik} & w_{Hi\,Ik}\end{bmatrix}^T$, $\mathbf{w}_{Hi\,k}^{o}=\begin{bmatrix} w_{Hi\,k} & \Delta w_{Hi\,k}\end{bmatrix}^T$, $i=\overline{1,2}$ with w_{Hik} is the reference input, $w_{Hi\,Ik}$ is the integral of reference input, $w_{Hi\,Ik}=w_{Hi\,Ik-1}+w_{Hi\,k}$, $\Delta w_{Hi\,k}=w_{Hi\,k}-w_{Hi\,k-1}$ is the increment of reference input; $\mathbf{e}_{Hi\,Ik}^{j}=\begin{bmatrix} e_{Hi\,k} & e_{Hi\,Ik}\end{bmatrix}^T$, $\mathbf{e}_{Hi\,k}^{o}=\begin{bmatrix} e_{Hi\,k} & \Delta e_{Hi\,k}\end{bmatrix}^T$, $i=\overline{1,2}$ with: $e_{Hi\,k}$ is the control error, $e_{Hi\,Ik}$ is the integral of control error, $e_{Hi\,Ik}=e_{Hi\,Ik-1}+e_{Hi\,k}$, Δe_{Hik} is the increment of control error; the output vectors are $\mathbf{y}_{Hi\,k}^{j}=\begin{bmatrix} y_{Hi\,k} & y_{Hi\,Ik}\end{bmatrix}^T$, $\mathbf{y}_{Hi\,k}^{o}=\begin{bmatrix} y_{Hi\,k} & \Delta y_{Hi\,k}\end{bmatrix}^T$, $i=\overline{1,2}$ with: y_{Hik} is the controlled output, $y_{Hi\,Ik}$ is the integral of controlled output, $y_{Hi\,Ik}=y_{Hi\,Ik-1}+y_{Hi\,k}$, $\Delta y_{Hi\,k}=y_{Hi\,k}-y_{Hi\,k-1}$ is the increment of controlled output; $\mathbf{u}_{ik}^{j}=\begin{bmatrix} u_{ik} & u_{f\,ik}\end{bmatrix}^T$, $\mathbf{u}_{ik}^{o}=\begin{bmatrix}\Delta u_{ik} & \Delta u_{fik}\end{bmatrix}^T$, $i=\overline{1,2}$ where $u_{f\,ik}$ represents the fictitious control signal, $\Delta u_{f\,ik}$ stands for the fictitious increment of control signal (Precup and Preitl, 1997; Precup and Preitl, 2003a).

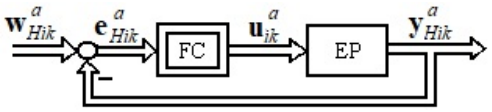

Figure 6: Modified structure of fuzzy control system.

The FC block is characterised by the nonlinear input-output static map **F**

$$\mathbf{F}: R^2 \to R^2, \mathbf{F}(\mathbf{e}_k^a)=\begin{bmatrix} f(\mathbf{e}_k^a) & 0\end{bmatrix}^T \tag{9}$$

where f ($f: R^2 \to R$) is the input-output static map of the nonlinear blocks (FC).

The state-space mathematical models can be expressed in terms of the following unified expression for both PI fuzzy controllers:

$$\begin{aligned} \mathbf{x}_{Hi\,k+1}^{a} &= \mathbf{A}^{a}\mathbf{x}_{Hi\,k}^{a}+\mathbf{B}^{a}\mathbf{u}_{ik}^{a} \\ \mathbf{y}_{Hik}^{a} &= \mathbf{C}^{a}\mathbf{x}_{Hi\,k}^{a}\end{aligned} \tag{10}$$

by inserting additional state variables, which result in the augmented state vectors $\mathbf{x}_{Hik}^{j}=\begin{bmatrix}\mathbf{x}_{Hik} & x_{y\,Hik}^{j}\end{bmatrix}^T$ for PI-FC-II and $\mathbf{x}_{Hik}^{o}=\begin{bmatrix}\mathbf{x}_{Hik} & x_{u\,Hik} & x_{y\,Hik}^{o}\end{bmatrix}^T$ for PI-FC-OI, due to the presence of the additional linear dynamics transferred from the PI fuzzy controller structures (Precup and Preitl, 1997; Precup and Preitl, 2003a). Therefore the resulting state-space matrices in case of PI-FC-II are

$$\begin{aligned} &\mathbf{A}^{j}=\begin{bmatrix}\mathbf{A} & \mathbf{0}\\ \mathbf{c}^T\mathbf{A} & 1\end{bmatrix}, \mathbf{B}^{j}=\begin{bmatrix}\mathbf{b} & \mathbf{1}\\ \mathbf{c}^T\mathbf{b} & 1\end{bmatrix}, \\ &\mathbf{C}^{j}=\begin{bmatrix}\mathbf{c}^T & 0\\ \mathbf{0}^T & 1\end{bmatrix} \\ &\mathbf{A}^{j}\in\Re^{n^j x n^j}, \mathbf{B}^{j}\in\Re^{n^j x 2},, \mathbf{C}^{j}\in\Re^{2 x n^j}\end{aligned} \tag{11}$$

and in case of PI-FC-OI are

$$\begin{aligned} &\mathbf{A}^{o}=\begin{bmatrix}\mathbf{A} & \mathbf{b} & \mathbf{0}\\ \mathbf{0}^T & 1 & 0\\ \mathbf{c}^T & 0 & 0\end{bmatrix}, \mathbf{B}^{o}=\begin{bmatrix}\mathbf{b} & \mathbf{1}\\ 1 & 1\\ 0 & 1\end{bmatrix} \\ &\mathbf{C}^{o}=\begin{bmatrix}\mathbf{c}^T & 0 & 0\\ \mathbf{c}^T & 0 & -1\end{bmatrix}, \\ &\mathbf{A}^{o}\in\Re^{n^o x n^o}, \mathbf{B}^{o}\in\Re^{n^o x 2}, \mathbf{C}^{o}\in\Re^{2 x n^o}\end{aligned} \tag{12}$$

where $n^j=n+1, n^o=n+2$ and n is the order of the mathematical models.

The structure presented in Fig. 7 is used in the stability analysis of the nonlinear control system, where the NL block represents a static nonlinearity due to the nonlinear part without dynamics of the FC block.

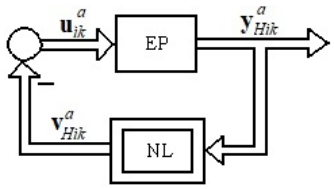

Figure 7: Structure of nonlinear control system involved in stability analysis.

The connections between the variables of the control system structures in Figs. 6 and 7 are

$$\mathbf{v}^a_{Hik} = -\mathbf{u}^a_{ik} = -\mathbf{F}(\mathbf{e}^a_{Hik}), \mathbf{y}^a_{Hik} = -\mathbf{e}^a_{Hik} \quad (13)$$

where the second component of $\mathbf{F}$ is always zero in order to neglect the effect of fictitious control signal.

The second equation in (10) is next expressed as follows using (13):

$$\mathbf{e}^a_{Hik} = -\mathbf{C}^a \mathbf{u}^a_{ik}, \mathbf{x}^a_{Hik} = \mathbf{C}^b \mathbf{e}^a_{Hik} \quad (14)$$

where the matrix $\mathbf{C}^b$, ($\mathbf{C}^b \in \Re^{n^a x 2}$), can be computed relatively easily as function of $\mathbf{C}^a$.

The proposed stability analysis method can be stated in terms of the following theorem:

Theorem. The nonlinear system, from Fig. 7 and with the mathematical model (10), is globally asymptotically stable if the three matrices $\mathbf{P}$ (positive definite, $\mathbf{P} \in \Re^{n^a x n^a}$), $\mathbf{L}$ (regular, dim $\mathbf{L} \in \Re^{n^a x n^a}$) and $\mathbf{V}$ (any, $\mathbf{V} \in \Re^{n^a x 2}$) fulfil the requirements I and II:

I.

$$\begin{aligned} (\mathbf{A}^a)^T \mathbf{P} \cdot \mathbf{A}^a &= -\mathbf{L}\,\mathbf{L}^T \\ \mathbf{C}^a - (\mathbf{B}^a)^T \mathbf{P} \cdot \mathbf{A}^a &= \mathbf{V}^T \mathbf{L}^T \\ -(\mathbf{B}^a)^T \mathbf{P} \cdot \mathbf{B}^a &= \mathbf{V}^T \mathbf{V} \end{aligned} \quad (15)$$

II. By introducing the matrices $\mathbf{M}$ ($\mathbf{M} \in \Re^{2x2}$), $\mathbf{N}$ ($\mathbf{N} \in \Re^{2x2}$) and $\mathbf{R}$ ($\mathbf{R} \in \Re^{2x2}$) defined as follows:

$$\begin{aligned} \mathbf{M} &= (\mathbf{C}^b)^T (\mathbf{L}\,\mathbf{L}^T - \mathbf{P}) \mathbf{C}^b \\ \mathbf{N} &= (\mathbf{C}^b)^T [\mathbf{L}\,\mathbf{V} - (\mathbf{A}^a)^T \mathbf{P}\,\mathbf{B}^a - 2(\mathbf{C}^a)^T \\ \mathbf{R} &= \mathbf{V}^T \mathbf{V} \end{aligned} \quad (16)$$

the inequality

$$f(\mathbf{e}^a_{Hik}) \mathbf{n}^T \mathbf{e}^a_{Hik} + (\mathbf{e}^a_{Hik})^T \mathbf{M}\, \mathbf{e}^a_{Hik} \geq 0 \quad (17)$$

holds for any value of the control error e_{Hik}, with the vector $\mathbf{e}^a_{Hik}$ defined in (13) and $\mathbf{n}$ – the first column in $\mathbf{N}$.

Proof. The condition I is the first equation in Kalman-Szegö's lemma, therefore it is fulfilled immediately (Landau, 1979).

In order to fulfil the condition II, the Popov inequality (17), which ensures the global asymptotic stability of the nonlinear control system, Fig. 7, for any positive constant β_0, is expressed as

$$S(k_1) = \sum_{k=0}^{k_1} (\mathbf{v}^a_{Hik})^T \mathbf{y}^a_{Hik} \geq -\beta_0^2, \forall k_1 \in N^* \quad (18)$$

Considering (13), the Popov sum $S(k_1)$ in (18) is transformed in

$$S(k_1) = -\sum_{k=0}^{k_1} (\mathbf{u}^a_{ik})^T \mathbf{y}^a_{Hik} \quad \forall k_1 \in N^* \quad (19)$$

Substituting the expressions of $\mathbf{x}^a_{Hik+1}$ and $\mathbf{y}^a_{Hik}$ according to (10) in (19), followed by adding and subtracting the term $(\mathbf{x}^a_{Hik+1})^T \mathbf{P} \cdot \mathbf{x}^a_{Hik+1}$ and using the properties of matrix transposition, the Popov sum $S(k_1)$ becomes

$$\begin{aligned} S(k_1) = -\sum_{k=0}^{k_1} \{ & -(\mathbf{x}^a_{Hik})^T (\mathbf{A}^a)^T \mathbf{P} \cdot \mathbf{A}^a \mathbf{x}^a_{Hik} \\ & -(\mathbf{x}^a_{Hik})^T [(\mathbf{A}^a)^T (\mathbf{P} + \mathbf{P}^T) \mathbf{B}^a + \\ & (\mathbf{C}^a)^T] \mathbf{u}^a_{ik} - (\mathbf{u}^a_{ik})^T (\mathbf{B}^a)^T \mathbf{P} \cdot \mathbf{B}^a \cdot \mathbf{u}^a_{ik} \\ & + (\mathbf{x}^a_{Hi\,k+1})^T \mathbf{P} \cdot \mathbf{x}^a_{Hi\,k+1}] \} \quad \forall k_1 \in N^* \end{aligned} \quad (20)$$

Replacing the expressions of $(\mathbf{A}^a)^T \mathbf{P} \cdot \mathbf{A}^a$, $(\mathbf{A}^a)^T \mathbf{P}^T \cdot \mathbf{B}^a$ and $(\mathbf{B}^a)^T \mathbf{P} \cdot \mathbf{B}^a$ in terms of (I), expressing $\mathbf{x}^a_{Hik}$ in accordance with (14) and using II, another form of the Popov sum $S(k_1)$ is obtained:

$$\begin{aligned} S(k_1) = & -\sum_{k=0}^{k_1} (\mathbf{x}^a_{Hi\,k+1})^T \mathbf{P} \cdot \mathbf{x}^a_{Hi\,k+1} + \\ & + \sum_{k=0}^{k_1} [(\mathbf{e}^a_{Hik})^T \mathbf{M} \cdot \mathbf{e}^a_{Hik} + (\mathbf{e}^a_{Hik})^T \mathbf{N} \cdot \mathbf{u}^a_{ik} \\ & + (\mathbf{u}^a_{ik})^T \mathbf{R} \cdot \mathbf{u}^a_{ik}] \quad \forall k_1 \in N^* \end{aligned} \quad (21)$$

Using the expression of $\mathbf{u}^a_{ik}$ from (13), the sum in (21) is expressed as

$$\begin{aligned} S(k_1) = & -\sum_{k=0}^{k_1} (\mathbf{x}^a_{Hi\,k+1})^T \mathbf{P} \cdot \mathbf{x}^a_{Hi\,k+1} \\ & + \sum_{k=0}^{k_1} [(\mathbf{e}^a_{Hi\,k})^T \mathbf{M} \cdot \mathbf{e}^a_{Hi\,k} + (\mathbf{e}^a_{Hi\,k})^T \mathbf{N} \cdot \mathbf{F}(\mathbf{e}^a_{Hi\,k}) \\ & + \mathbf{F}^T (\mathbf{e}^a_{Hi\,k}) \mathbf{R} \cdot \mathbf{F}(\mathbf{e}^a_{Hi\,k})] \quad \forall k_1 \in N^* \end{aligned} \quad (22)$$

Finally, the expression of the sum $S(k_1)$ is obtained by using $\mathbf{F}$ from (9) and the positive element r_{11} of the matrix $\mathbf{R}$:

$$S(k_1) = -\sum_{k=0}^{k_1} [(\mathbf{x}^a_{Hi\,k+1})^T \mathbf{P} \cdot \mathbf{x}^a_{Hi\,k+1} + r_{11} f^2(\mathbf{e}^a_{Hi\,k})] + \sum_{k=0}^{k_1} [(\mathbf{e}^a_{Hi\,k})^T \mathbf{M} \cdot \mathbf{e}^a_{Hi\,k} + f(\mathbf{e}^a_{Hi\,k})\mathbf{n}^T \cdot \mathbf{e}^a_{Hi\,k}] \;\; \forall k_1 \in N^* \quad (23)$$

Both sums in the right-hand term of (23) are positive and therefore the sum $S(k_1)$ is also positive, which means that the condition II guarantees the fulfilment of the Popov inequality (18).

In conclusion, the fuzzy control system is globally asymptotically stable.

For $n > 2$, only the matrix $\mathbf{P}$ in (I is important for the fuzzy CS stability analysis because the matrices $\mathbf{M}$, $\mathbf{N}$ and $\mathbf{R}$ in II can be expressed as functions of $\mathbf{P}$:

$$\begin{aligned} \mathbf{M} &= -(\mathbf{C}^b)^T (\mathbf{A}^a)^T \mathbf{P} \cdot \mathbf{A}^a \mathbf{C}^b \\ \mathbf{N} &= -(\mathbf{C}^b)^T [(\mathbf{A}^a)^T (\mathbf{P} + \mathbf{P}^T)\mathbf{B}^a \\ &\quad + (\mathbf{C}^a)^T] \\ \mathbf{R} &= -(\mathbf{B}^a)^T \mathbf{P} \cdot \mathbf{B}^a \end{aligned} \quad (24)$$

4 EXPERIMENTAL RESULTS

This section is dedicated to test and validate the two proposed control structures, presented above by real-time experimental results. The parameters of the MIMO–PI–FC–II that ensure the stability of the fuzzy control system are tuned as: $B_{eH1} = 0.15$, $B_{eIH1} = 1.08 \cdot 10^3$, $B_{uH1} = 0.6$, $B_{eH2} = 0.37$, $B_{eIH2} = 1.85 \cdot 10^3$, $B_{uH2} = 0.36$. The parameters of MIMO–PI–FC–OI that ensure the stability of the fuzzy control system are tuned as: $B_{eH1} = 0.27$, $B_{\Delta eH1} = 1.88 \cdot 10^{-5}$, $B_{\Delta uH1} = 7.05 \cdot 10^{-4}$, $B_{eH2} = 0.45$, $B_{\Delta eH2} = 3.13 \cdot 10^{-5}$, $B_{\Delta uH2} = 7.83 \cdot 10^{-5}$.

The following testing scenario was considered and conducted: the two proposed control structures were tested on the time frame of 1000 s with step–type reference inputs which were set to $w_{Hik} = 0.1m$, $i = \overline{1,2}$ and are plotted in Fig. 8 and Fig. 9, respectively, for both proposed CSs.

The tracking errors e_{Hik} for both the MIMO–PI–FC–II–CS and MIMO–PI–FC–OI–CS are in fact the control errors defined in Fig. 5. The mean square error (MSE) was also calculated for both CSs as

$$\mathrm{J}_{\mathrm{MSE}_{Hi}} = \frac{1}{N} \sum_{t_d=1}^{N} (e_{Hik}(t_d))^2, \;\; i = \overline{1,2} \quad (25)$$

where $N = 100001$ is the number of records, and the obtained values are given in Table 2.

The conclusion drawn by analyzing the plots given in Figs. 8 and 9, and after comparing the results presented in Table 2, is that the zero steady state control error is ensured for H_1 and H_2 in both the proposed CSs and the best performances indices in terms of settling time, rise time and mean square error are obtained in case of MIMO-PI-FC-OI-CS.

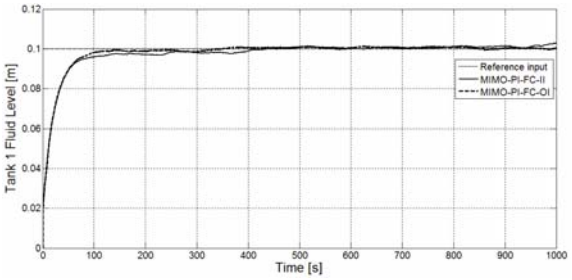

Figure 8: Tank 1 fluid levels (H_1) versus time (t) in case of MIMO-PI-FC-II-CS and MIMO-PI-FC-OI-CS.

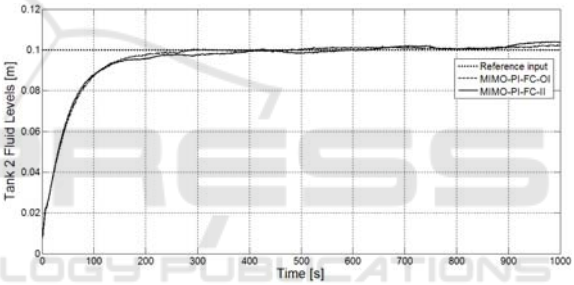

Figure 9: Tank 2 fluid levels (H_2) versus time (t) in case of MIMO-PI-FC-II-CS and MIMO-PI-FC-OI-CS.

Table 2: Mean Square Errors.

$\mathrm{J}_{\mathrm{MSE}_{Hi}}, i = \{1,2\}$	$\mathbf{H_1}$	$\mathbf{H_2}$
MIMO–PI–FC-II	$0.8379 \cdot 10^{-4}$	$0.2208 \cdot 10^{-3}$
MIMO–PI–FC-OI	$0.8 \cdot 10^{-4}$	$0.2190 \cdot 10^{-3}$

5 CONCLUSIONS

This paper has presented the design and validation of two CSs applied to level control of V2TS. The first CS structure consists of a Multi Input Multi Output Proportional Integral Fuzzy Controller with integration of controller input (MIMO–PI–FC–II) and the second CS structure consists of a Multi Input Multi Output Proportional Integral Fuzzy Controller with integration of controller output (MIMO–PI–FC–OI).The proposed control solutions were tested in the same scenarios and their control performance is given

in Table 2. The experimental results prove that the best performances indices in terms of settling time, rise time and mean square error are obtained in case of MIMO-PI-FC-OI-CS.

Future research will be focused on the improvement of the performance indices by designing CSs with hybrid structures applied to mechatronics systems that include large-scale complex systems (Filip, 2008), robotics and autonomous systems (Haidegger et al., 2012; Blažič, 2014; Kovács et al., 2016), model predictive control (Bouzouita et al., 2008, Landau, 1979, Mirzaee and Salahshoor, 2012), fuzzy models and control (Precup and Preitl, 2003b; Precup et al., 2013; Johanyák, 2015; Olivas et al., 2017; Vrkalovic et al., 2018), engines (Andoga et al., 2018), cognitive models (Sánchez Boza et al., 2011; Direito et al., 2017; Ferreira et al., 2017; Braga et al., 2019), and chaotic systems (Precup et al., 2014; Köse and Mühürcü, 2018).

ACKNOWLEDGEMENTS

This work was supported by the CNFIS-FDI-2019-0696 project of the Politehnica University of Timisoara, Romania.

REFERENCES

Andoga, R., Főző, L., Judičák, J., Bréda, R., Szabo, S., Rozenberg, R., Džunda, M., 2018. Intelligent situational control of small turbojet engines. *International Journal of Aerospace Engineering*, 2018, paper 8328792, 1-16.

Blažič, S., 2014. On periodic control laws for mobile robots. *IEEE Transactions on Industrial Electronics*, 61(7), 3660-3670.

Braga, D., Madureira, A. M., Coelho, L., Ajith, R., 2019. Automatic detection of Parkinson's disease based on acoustic analysis of speech. *Engineering Applications of Artificial Intelligence*, 77, 148-158.

Bojan-Dragos, C.-A., Szedlak-Stinean, A.-I., Precup, R.-E., Grugui, L., Hedrea, E.-L., Mituletu, I.-C., 2018. Control solutions for vertical three-tank systems, in *Proceedings of IEEE 13th International Symposium on Applied Computational Intelligence and Informatics*, Timisoara, Romania, 593-598.

Bouzouita, B., Bouani, F., Wertz, W., Ksouri, M., 2008. Implementation of SISO robust predictive control to a three tanks system, in *Proceedings of. IEEE International Conference on Control Applications*, San Antonio, TX, USA, 323-328.

Chakravarthi, M. K., Pannem, V. K, Venkatesan, N., 2014. Real time implementation of gain scheduled controller design for higher order nonlinear system using LabVIEW, *International Journal of Engineering and Technology*, 6(5), 2031-2038.

Dinesh Kumar, D., Meenakshipriya, B., 2012. Design and implementation of non linear system using gain scheduled PI controller, *Procedia Engineering*, 38, 3105-3112.

Direito, B., Teixeira, C. A., Sales, F., Castelo-Branco, M., Dourado, A., 2017. A realistic seizure prediction study based on multiclass SVM. *International Journal of Neural Systems*, 27(3), 1-15.

Dormido, R., Vargas, H., Duro, N., Sanchez, J., Dormido-Canto, S., Farias, G., Esquembre, F., Dormido, S., 2008. Development of a web-based control laboratory for automation technicians: the three-tank system, *IEEE Transactions on Education*, 51, 35-44.

Ferreira, R., Graça Ruano, M., Ruano, A. E., 2017. Intelligent non-invasive modeling of ultrasound-induced temperature in tissue phantoms. *Biomedical Signal Processing and Control*, 33, 141-150.

Filip, F. G., 2008. Decision support and control for large-scale complex systems, *Annual Reviews in Control*, 32(1), 61-70.

Haidegger, T., Kovács, L., Precup, R.-E., Benyó, B., Benyó, Z., Preitl, S., 2012. Simulation and control for telerobots in space medicine, *Acta Astronautica*, 181(1), 390-402.

Inteco, *Multitank System, User's Manual*. Krakow, Poland: Inteco Ltd., 2007.

Johanyák, Z. C., 2015. A simple fuzzy logic based power control for a series hybrid electric vehicle, in *Proceedings of 9th IEEE European Modelling Symposium on Mathematical Modelling and Computer Simulation*, Madrid, Spain, 207-212.

Köse, E., Mühürcü, A., 2018. The control of brushless DC motor for electric vehicle by using chaotic synchronization method, *Studies in Informatics and Control*, 27(4), 403-412.

Kovács, B., Szayer, G., Tajti, F., Burdelis, M., Korondi, P., 2016. A novel potential field method for path planning of mobile robots by adapting animal motion attributes, *Robotics and Autonomous Systems*, 82, 24-34.

Landau, I.D., 1979. *Adaptive Control*, New York, Marcel Dekker, Inc.

Mirzaee, A., Salahshoor, K., 2012. Fault diagnosis and accommodation of nonlinear systems based on multiple-model adaptive unscented Kalman filter and switched MPC and H_∞ loop-shaping controller, *Journal of Process Control*, 22(3), 626-634.

Na, J., Ren, X., Shang, C., Guo, Y., 2012. Adaptive neural network predictive control for nonlinear pure feedback systems with input delay, *Journal of Process Control*, 22(1), 194-206.

Olivas, F., Valdez, F., Castillo, O., González, C. I., Martinez, G. E., Melin, P., 2017. Ant colony optimization with dynamic parameter adaptation based on interval type-2 fuzzy logic systems. *Applied Soft Computing*, 53, 74-87.

Orani, N., Pisano, A., Usai, E., 2009. Fault detection and reconstruction for a three-tank system via high-order sliding-mode observer, in *Proceedings of IEEE*

International Conference on Control Applications, Saint Petersburg, Russia, 1714-1719.

Popov, V. M., 1973. *Hyperstability of Control Systems*, Berlin, Heidelberg, New York, Springer-Verlag.

Precup, R.-E., Preitl, S., 1997. Popov-type stability analysis method for fuzzy control systems, in *Proceedings of Fifth European Congress on Intelligent Technologies and Soft Computing (EUFIT)*, 2, Aachen, Germany, 1306-1310.

Precup, R.-E., Preitl, S., 2003a. Popov-type stability analysis method for fuzzy control systems with PI fuzzy controllers, *Revue Roumaine de Sciences Techniques, Electrotechnique et Energetique Series*, 48(4), 505-522.

Precup, R.-E., Preitl, S., 2003b. Development of fuzzy controllers with non-homogeneous dynamics for integral-type plants, *Electrical Engineering*, 85(3), 155-168.

Precup, R.-E., Mosincat, I., Radac, M.-B., Preitl, S., Kilyeni, S., Petriu, E.-M., Dragos, C.-A., 2010. Experiments in iterative feedback tuning for level control of three-tank system, in *Proceedings of the 15th IEEE Mediterranean Electrotechnical Conference*, Valletta, Malta, 564-569.

Precup, R.-E., Tomescu, M.-L., Dragos, C.-A., 2014. Stabilization of Rössler chaotic dynamical system using fuzzy logic control algorithm, *International Journal of General Systems*, 43(5), 413-433.

Precup, R.-E., Tomescu, M. L., Preitl, S., Petriu, E. M., Fodor, J., Pozna, C., 2013. Stability analysis and design of a class of MIMO fuzzy control systems, *Journal of Intelligent & Fuzzy Systems*, 25(1), 145-155.

Sánchez Boza, A., Haber Guerra, R., Gajate, A., 2011. Artificial cognitive control system based on the shared circuits model of sociocognitive capacities. A first approach. *Engineering Applications of Artificial Intelligence*, 24(2), 209-219.

Vrkalovic, S., Lunca, E.-C., Borlea, I.-D., 2018. Model-free sliding mode and fuzzy controllers for reverse osmosis desalination plants. *International Journal of Artificial Intelligence*, 16(2), 208-222.